White matter structure assessment from reduced HARDI data using low-rank polynomial approximations

Yaniv Gur⋆, Fangxiang Jiao⋆, Stella Xinghua Zhu† and Chris R. Johnson⋆

⋆ SCI Institute, University of Utah, 72 S. Central Campus Dr., SLC, UT 84112, USA
† Department of Computer Science, The University of Hong Kong, Pokfulam Road, Hong Kong

Abstract. Assessing white matter fiber orientations directly from DWI measurements in single-shell HARDI has many advantages. One of these advantages is the ability to model multiple fibers using fewer parameters than are required to describe an ODF and, thus, reduce the number of DW samples needed for the reconstruction. However, fitting a model directly to the data using Gaussian mixture, for instance, is known as an initialization-dependent unstable process. This paper presents a novel direct fitting technique for single-shell HARDI that enjoys the advantages of direct fitting without sacrificing the accuracy and stability even when the number of gradient directions is relatively low. This technique is based on a spherical deconvolution technique and decomposition of a homogeneous polynomial into a sum of powers of linear forms, known as a *symmetric tensor decomposition*. The fiber-ODF (fODF), which is described by a homogeneous polynomial, is approximated here by a discrete sum of even-order linear-forms that are directly related to rank-1 tensors and represent single-fibers. This polynomial approximation is convolved to a single-fiber response function, and the result is optimized against the DWI measurements to assess the fiber orientations and the volume fractions directly. This formulation is accompanied by a robust iterative alternating numerical scheme which is based on the Levenberg-Marquardt technique. Using simulated data and in vivo, human brain data we show that the proposed algorithm is stable, accurate and can model complex fiber structures using only 12 gradient directions.

1 Introduction

In contrast to diffusion tensor imaging (DTI), High Angular Resolution Diffusion Imaging (HARDI) is an imaging technique that is capable of describing complex white matter structures such as crossing fibers. Given HARDI data, various reconstruction techniques are used to infer the fiber structures [1–6]. These techniques are primarily based on the reconstruction of an orientation distribution function (ODF) that describes the dominant diffusion directions. To recover the white matter fiber pathways, the dominant diffusion directions are extracted from the ODF. Since white matter connectivity maps are obtained from tracking these directions, an accurate reconstruction of this information is crucial. This motivated the development of various analytical and numerical techniques to achieve this task. These techniques are mainly based on polynomial root-finding and high order ODF tessellation [7–9], or low-rank tensor approximations [10, 11]. However, the accuracy of these algorithms is limited by the ODF quality of reconstruction and its reconstruction order (i.e., the spherical harmonics truncation order). Also, since these algorithms introduce significant complexity, the complete process of ODF reconstruction, followed by orientations estimation, is inefficient. Multi-compartment models [3, 12–14], however, avoid the ODF estimation step by estimating the fiber parameters directly from the DWI measurements. This allows modeling multiple fiber orientations using a few number of parameters and, thus, reduce the number of DWI measurements needed for the reconstruction.

However, these models have two main disadvantages: First, to obtain the best results the correct number of fiber compartments has to be pre-selected. As was pointed out in [13], in single-fiber voxels the model will lose accuracy if fitting two-compartments to the data. Second, the resulting non-linear optimization problem is unstable and initialization dependent since the objective function possesses local minima.

In this paper we present an alternative direct estimation technique that enjoys the advantages of direct fitting without sacrificing the stability, accuracy and robustness to noise of the algorithm. In addition, it allows accurate estimation of the orientations even in a case of over-fitting. This technique is based on spherical deconvolution, which is a powerful technique for modelling complex fiber structures by means of a fiber-ODF (fODF) [2]. It is known that the maximal accuracy of spherical deconvolution is achieved when the fODF is decomposed into rank-1 tensors that represent single fiber orientations [10, 11, 15]. Thus, the fODF estimation step is followed by a tensor decomposition. In this work we show that using rank-1 tensor fiber representations as linear-forms, these two distinct steps can be combined into one optimization problem that allows robust estimation of the fiber parameters directly from the DWI measurements.

The proposed approach is motivated by the *symmetric tensor decomposition* [16], that is, any homogeneous polynomial of order d may be decomposed into a sum of r distinct linear-forms of the same order. Since any spherical function with antipodal symmetry may be represented as an even-order homogeneous polynomial (or a symmetric higher-order tensor) [17], we can decompose an ODF or a fODF in a similar manner. Thus, we consider here a lower-rank polynomial approximation of a fODF in terms of even order linear-forms which are directly related to rank-1 tensors. In this approximation, each linear-form represents a single fiber and its coefficients correspond directly to the fiber orientation and the volume fraction (the mixing parameter). Similar to existing multi-compartment models, the fODF expansion in linear-forms is naturally positive-definite, and hence, no additional constraint that guarantees this property is required. The expansion's coefficients are estimated via a spherical deconvolution operation such that each term is convolved to a single-fiber response and the result is optimized against the HARDI measurements by means of the l_2 norm. The resulting non-linear optimization problem is solved here using a novel iterative alternating scheme based upon the Levenberg-Marquardt technique and is shown to produce stable and accurate results.

In this paper we test the algorithm on simulated data as well as in vivo, human brain data. In both cases the set of gradient directions was sub-sampled from 96 (or 64 for the human brain data) down to 12 so we could explore the limitations of the algorithm and the decline in performance. We show that, in both cases (simulated and real data), sub-sampling from 64 to 32 directions does not change significantly the results. A performance decline is clearly observed when the set contains only 12 gradient directions, yet, the algorithm produces useable results and can reliably separate fibers crossing at 75 degrees and above.

This paper is organized as follows: In Sec. 2 we briefly review the spherical deconvolution approach and develop the new method in this context. In Sec. 3 we discuss the numerical optimization technique that we developed to solve the minimization problem. Finally, Sec. 4 is devoted to accuracy and stability studies and experiments on in-vivo, human brain data.

2 Spherical deconvolution via symmetric tensor decomposition

Spherical deconvolution is a common technique to recover major diffusion directions from DWI data [2]. It is based on a convolution between a spherically symmetric function, known as fODF, and an axially symmetric kernel that represents a single fiber response. Given a vector of n DWI measurements in the gradient directions, the fODF, denoted by F, is reconstructed by solving the following deconvolution problem:

$$\min_F \frac{1}{2} \sum_{i=1}^{n} \left\| S(\mathbf{g}_i, b) - S_0 \int_{S^2} F(\mathbf{v}) K(\mathbf{g}_i, \mathbf{v}) d\mathbf{v} \right\|^2 . \tag{1}$$

This problem is solved for a fixed kernel, K, where its width is adjusted to the particular dataset. The resulting fODF represents a sum of spherical delta functions aligned with the fiber orientations and weighted by the volume fractions. This basic problem is solved by means of least-squares where the fODF is reconstructed by a pseudo-inverse operation. However, additional constraints such as fODF positivity leads to non-linear optimization problem [2].

In [16] it was shown that any homogeneous polynomial of order d may be decomposed into a sum of linear-forms of the same order such that:

$$F(x_1, x_2, \dots, x_l) = \sum_{i=1}^{r} \lambda_i f_i^d \tag{2}$$

where $f_i = (\sum_{i=1}^{l} \alpha_i x_i)$, r is the polynomial *rank* and l is the polynomial *dimension*. This decomposition is known as *symmetric tensor decomposition* since homogeneous polynomials are directly related to symmetric tensors. An algorithm to decompose a general homogenous polynomial was proposed in [16].

It is known that any spherical function with antipodal symmetry may be represented as an even-order homogeneous polynomial, where its order is equivalent to the truncation order of the corresponding spherical harmonics expansion [17]. Since a fODF may be represented as a homogenous polynomial, one may use [16] to compute its full-rank decomposition. However, a full-rank fODF encodes information on white matter fibers, as well as noise. Thus, it was proposed in [10, 11] to recover the fiber orientations via a lower-rank tensor approximation. This approximation was applied to the fODF and required its estimation first.

To combine the fODF reconstruction and the orientations estimation into one optimization problem, we first approximate the fODF using an equivalent lower-rank approximation by means of polynomial approximation (symmetric tensor decomposition) such that:

$$F(\mathbf{v}) \sim \sum_{i=1}^{\tilde{r}} \gamma_i f_i^d = \sum_{i=1}^{\tilde{r}} (\boldsymbol{\alpha}_i \cdot \mathbf{v})^d, \quad \tilde{r} < r, \tag{3}$$

where $\boldsymbol{\alpha}_i \in \mathbb{R}^3$, $\mathbf{v} \in S^2$ and each fiber aligned in direction $\boldsymbol{\alpha}_i$ is identified with a linear form $(\boldsymbol{\alpha}_i \cdot \mathbf{v})^d$. The number of fibers to be estimated is determined by the approximation rank $\tilde{r}$ and the expansion coefficients are defined as $\gamma_i = \|\boldsymbol{\alpha}_i\|^d$.

Next, we substitute (3) into (1). This leads to the following non-linear optimization problem:

$$\min_{\boldsymbol{\alpha}_j} \frac{1}{2} \sum_{i=1}^{n} \left\| S(\mathbf{g}_i, b) - S_0 \int_{S^2} \sum_{j=1}^{\tilde{r}} (\boldsymbol{\alpha}_j \cdot \mathbf{v})^d K(\mathbf{g}_i, \mathbf{v}) d\mathbf{v} \right\|^2 . \tag{4}$$

This problem is solved for the coefficients of the linear-forms, three coefficients for each fiber, which are directly estimated from the DWI measurements. The fiber orientations and the volume fractions are derived as follows: Since each linear-form gets its maximum at the direction specified by $\boldsymbol{\alpha}_j$, given the optimal solution, $\tilde{\boldsymbol{\alpha}}_j$, the corresponding fiber orientation is simply $\mathbf{u}_j = \frac{\tilde{\boldsymbol{\alpha}}_j}{\|\tilde{\boldsymbol{\alpha}}_j\|}$. As we do not impose the constraint $\sum_{j=1}^{\tilde{r}} \|\boldsymbol{\alpha}_j\|^d = 1$, the corresponding volume fraction is given by $w_j = \frac{\|\tilde{\boldsymbol{\alpha}}_j\|^d}{\sum_{j=1}^{\tilde{r}} \|\tilde{\boldsymbol{\alpha}}_j\|^d}$.

3 Numerical optimization

To solve this non-linear optimization problem (4) we adopt the Levenberg-Marquardt (LM) technique. When $\tilde{r} = 1$, the three coefficients can be estimated accurately using a straightforward implementation of the LM. However, when $r > 1$, more coefficients are involved and estimating them at once provides poor results. To deal with the multi-fiber estimation case, we suggest an iterative alternating LM scheme. In this scheme, a complete update step is composed of $\tilde{r}$

LM sub-steps. In each sub-step only the coefficient associated with a single fiber are updated while the other coefficients are kept fixed as described in Algorithm 1. In each iteration, one has to convolve the fiber estimate to the kernel. This operation is performed using a discrete spherical integration scheme [18]. In terms of convergence, we have found that the algorithm is very robust and converges for any initial guess.

Algorithm 1 Alternating LM for $\tilde{r} = 2$

1: Let I be the objective function defined in 4, and let $J_k = \frac{\partial I}{\partial \boldsymbol{\alpha}_k}$, $k = 1, 2$..
2: Set $t = 0$.
3: Initialize $\boldsymbol{\alpha}_k^t$, $k = 1, 2$.
4: Compute $\boldsymbol{\alpha}_1^{t+1}$ using an LM update with respect to $J_1(\boldsymbol{\alpha}_1^t, \boldsymbol{\alpha}_2^t)$ and a damping parameter ϵ_1.
5: Compute $\boldsymbol{\alpha}_2^{t+1}$ using an LM update with respect to $J_2(\boldsymbol{\alpha}_1^{t+1}, \boldsymbol{\alpha}_2^t)$ and a damping parameter ϵ_2.
6: **if** converged **then**
7:     return $\boldsymbol{\alpha}_{1,2}^t$
8: **else**
9:     $t \leftarrow t + 1$
10:     goto 4
11: **end if**

4 Simulations

4.1 Synthetic data

To test the accuracy and stability of the algorithm we simulated two crossing fibers at 4 separation angles: 45, 60, 75 and 90, equal volume fractions and two b-values: $b = 1500 s \backslash mm^2$ and $b = 3000 s \backslash mm^2$. The signal was simulated using the multi-tensor model:

$$S(\mathbf{g}_i, b) = S_0 \sum_{j=1}^{2} w_j \exp\left(-b \mathbf{g}_i^T D_j \mathbf{g}_i\right) \tag{5}$$

where for each compartment we assume a prolate tensor with FA=0.8. The simulated signal was corrupted by Rician noise distribution as follows:

$$S_{\text{noisy}}(\mathbf{g}_i, b) = \sqrt{(S(\mathbf{g}_i, b) + n_1)^2 + n_2^2}. \tag{6}$$

where $n_1,\ n_2 \sim \mathcal{N}(0, \sigma^2)$ and $\sigma = \frac{S_0}{\text{SNR}}$.

For all of the experiments presented below the SNR was set to 20 and for each separation angle the performance of the algorithm was evaluated on 200 noise realizations. The polynomial order is set to $d = 8$ as this value gives an optimal trade-off between the ability to resolve low separation angles and noise sensitivity at this SNR [2]. The single-fiber response kernel is described here by the Watson function $K(\mathbf{g}_i, \mathbf{v}, \delta) = \exp\left(-\delta(\mathbf{g}_i^T \cdot \mathbf{v})^2\right)$ where δ is a function of the b-value and the principal diffusivity, $\mathbf{g}_i$ is the gradient direction and $\mathbf{v}$ is the integration parameter. The Watson distribution is preferred here to the Bingham distribution used in [19]. As was pointed out in [19] the Bingham distribution accounts better for fiber-spread but decreases the angular separation power of the algorithm which is not a desired result here.

All the angular deviations reported here are calculated by summing up the deviations of the fibers from their closest ground-truth compartments, and dividing the result by the number of fibers (two fibers in our experiments). In the first experiment we tested the stability of the algorithm using 64, 32 and 12 gradient directions. For each separation angle we simulated a noisy signal at different separation angle, initialized the algorithm randomly 200 times and measured the mean angular deviation from the true orientations as well as the standard deviation. The results in Fig. 1 show that the algorithm provides stable performance in all of the simulated cases using 64 and 32 directions. The stability of the algorithm declines when the number of gradient directions is reduced to 12. In that case, only large separation angles can be detected reliably, especially when b=3000.

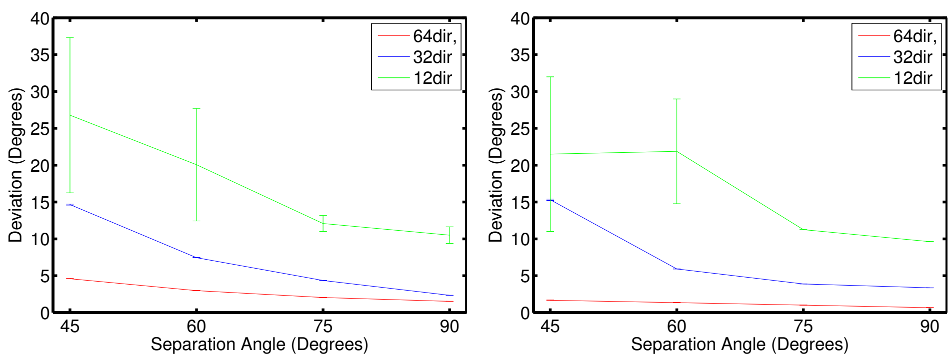

Fig. 1. Stability analysis for SNR=20. The experiments were carried on b=1500 (left) and b=3000 (right).

Next, we tested the accuracy of the algorithm. For each separation angle 200 noisy data instantiations were simulated and the angular deviation was measured separately for each instantiation. To test the performance decline under gradient directions sub-sampling, different sets of gradient directions were used: 96, 64, 32 and 12. The mean and the standard deviation of the collected results are depicted in Fig. 2. These results verify the stability test observations: The algorithm performs very well using 32 gradient directions and provide plausible results with only 12 gradient directions. Note that 12 directions are below the minimal number of measurements required for a 4th-order ODF estimation (15 coefficients) without using sparse representations or super-resolution techniques.

Finally, we compared our results to direct multi-tensor fitting. Since the signal was simulated using the multi-tensor model, theoretically, fitting this model to the data would give the best results. However, the comparison results depicted in Fig. 3 show that our algorithm is more stable, provide more accurate results and has a better separation resolution. To compare robustness to noise we added a dataset with SNR=40.

The multi-tensor fitting results were generated using Camino [20] with cylindrically symmetric tensors constraint. To get the best results, the diffusivities were set to the same values used to simulate the signal. The superiority of our algorithm in terms of accuracy and robustness to noise with only 12 samples is clearly shown in Fig. 3.

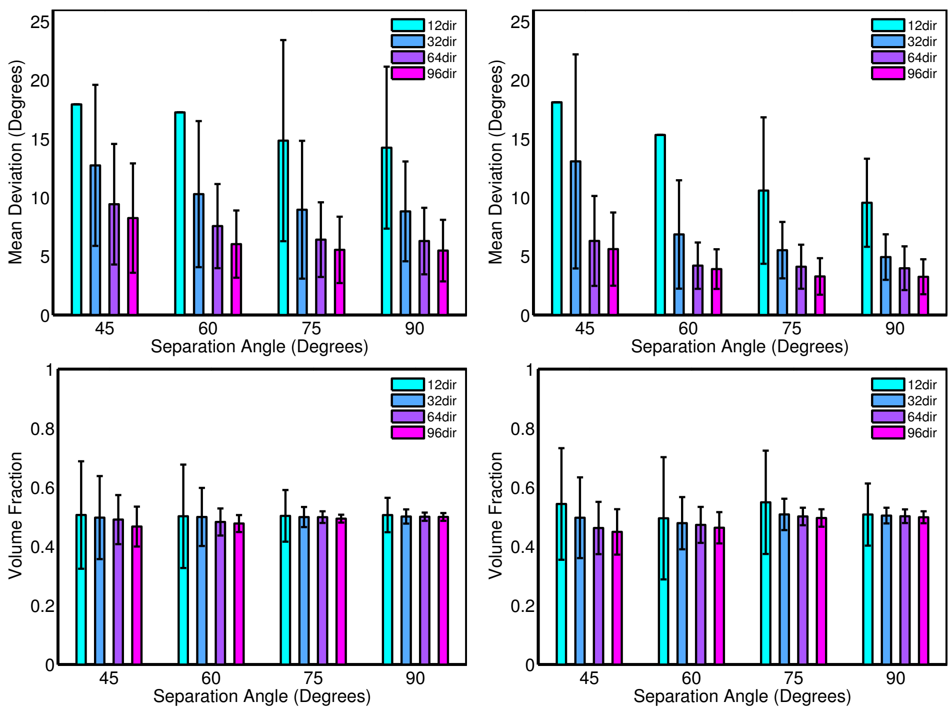

Fig. 2. Simulated data with SNR=20. Results of two b-values are presented: $1500s\backslash mm^2$ (left) and $3000s\backslash mm^2$ (right). The angular resolution is presented at the top and the volume fractions at the bottom. When the standard deviation exceeds the axis limit, we present the mean only.

In addition to the results reported here, our algorithm was compared with 12 different HARDI reconstruction techniques in ISBI'12 Workshop on HARDI

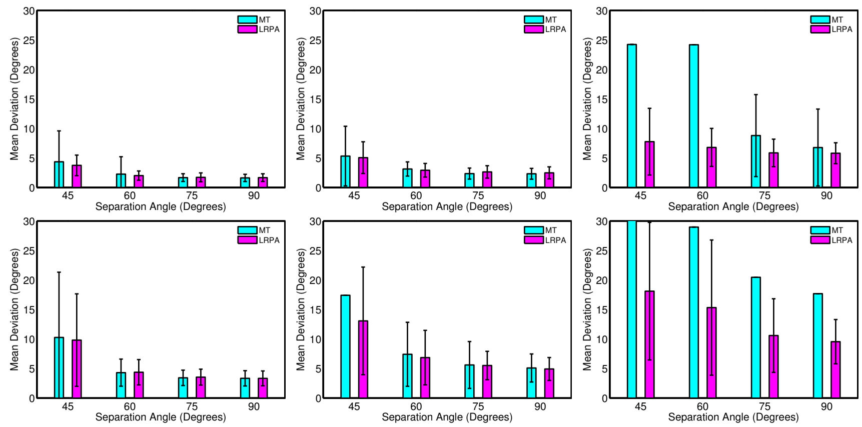

Fig. 3. Comparison of our Low Rank Polynomial Approximation (LRPA) and the Multi-Tensor (MT) model. The b-value is 3000 and the SNRs are 40 (top) and 20 (bottom). From left to right: 64, 32 and 12 gradient directions.

reconstruction [21]. The different algorithms were evaluated on a simulated 3D phantom as well as single voxels, in three SNR levels: 30, 20 and 10. Each algorithm was ranked based on the accuracy of fiber directions reconstruction, estimation of the number of fibers in each voxel and the ODF quality compared to the ground-truth. The number of gradient directions used for the reconstruction was also taken into account for the final ranking. Our algorithm (presented under the team name "The HOT gang") was ranked first or second in all of the three final ranking options.

The measured running time for a Matlab implementation of our algorithm is on average 40ms per voxel. This was measured on a standard laptop with 2.4Ghz Intel Core i5 CPU and 4 GM RAM. The tested implementation is non-optimal and acceleration methods can be used to achieve faster convergence times.

4.2 Human brain data

The human brain data was acquired on a 3T Siemens Tim Trio scanner using a single-shot spin-echo EPI sequence and a b-value of 2000 s/mm^2. One B0 image and 64 diffusion weighted images with a matrix size of $106 \times 106 \times 76$ and a voxel volume of $2\,\mathrm{mm}^3$ were acquired. The measured baseline SNR for these data was approximately 20. A white matter mask was registered to the data and the kernel width, δ, was estimated by computing the mean principal diffusivity of all white matter voxels with FA > 0.7.

Selecting the number of fiber compartments per voxel is a significant challenge, especially in direct model fitting techniques. As was pointed out in[13], fitting a mixture model with more than one compartment to a single fiber voxel will yield inaccurate results. Therefore, the number of fibers has to be pre-selected by using statistical inference methods such as an F-test. As we have found out

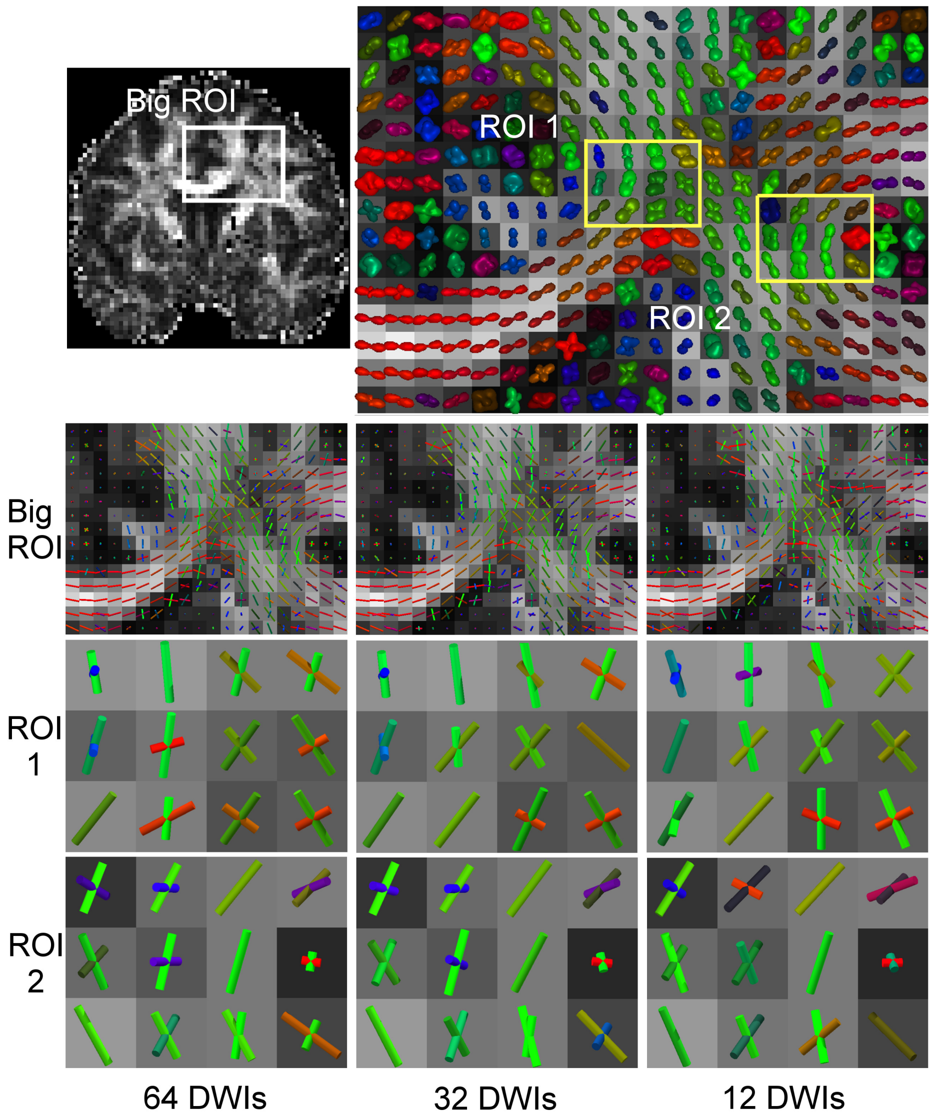

Fig. 4. Coronal slice showing reconstruction results of a crossing fibers region in human brain. From left to right: 64, 32 and 12 gradient directions. The FA values are shown at the background. The ODFs were reconstructed using [4] and are only provided as a reference for the fibers' structure in this ROI.

by simulated data experiments, our technique can accurately resolve the fiber orientations even in a case of over-fitting. That is, fitting a convolution of a sum of two linear-forms to a single fiber voxel, will yield a dominant fiber with a high volume fraction and a fiber with a low volume fraction. The dominant fiber accurately matches the orientation of the single fiber. This suggests that we can estimate the orientations everywhere using a fixed number of linear-forms and, then, eliminate "weak" fibers by direct thresholding. This is a clear advantage over multi-compartment fitting techniques. Also, it was shown in [14] that weight-based thresholding provides more accurate estimates of the number of fibers compared to statistical inference methods.

For this brain data we set $\tilde{r} = 3$ and learn the threshold from the high FA voxels that were used for the kernel parameter estimation. As most of these voxels lie in single tract regions, such as the corpus callosum, they presumably consist of single fibers. Thus, by applying a rank-two polynomial approximation to these voxels, the term with the lowest weight is likely to describe noise rather than a fiber. Indeed, the results show a high ratio between the weights of the first and the second term in these voxels. The threshold was then set as the average of the lowest weights where a value of 0.21 was computed. Thus, fibers with a volume fraction less than about 25% of the dominant volume fraction are considered as noise and eliminated.

To test the algorithm we have chosen the brain region where the corpus callosum (CC), the corona radiata (CR) and the superior longitudinal fasciculus (SLF) form a crossing pattern (Fig. 4). The results show that along the single tracts mostly one fiber model was selected whereas in the region where the different tracts cross, mostly two-fiber patterns were selected.

The fiber orientations were reconstructed using different sets of gradient directions which contain 64, 32 and 12 directions. The original set of gradient directions was sub-sampled using the algorithm described in [22]. The results of the fiber orientations and the number of fiber selected in each voxel are very similar whether 64 or only 32 directions were used. Crossing fibers are still presented using only 12 gradient directions although a performance decline is observed. This is due to loss of separation resolution and estimation accuracy in compliance with the simulated data observations. Yet, considering the noise level and the number of gradient directions used, these results are plausible. Note that we have not used any spatial regularization term in the current algorithm and we believe that these results can be improved by adding such regularization.

5 Conclusions

We presented a robust technique for the estimation of white matter fiber orientations and volume fractions directly from single-shell HARDI measurements. Similar to multi-compartment models, this technique avoids the complexity of extracting the orientations from the ODF and can model complex fiber structures using a few number of parameters. This technique relies on a low-rank homogeneous polynomial approximation by means of powers of linear-forms representing single fibers. An l_2 optimization problem based on a spherical deconvolution technique is used to estimate the fiber orientations and the volume fractions. Our technique is accompanied by a robust iterative alternating Levenberg-Marquardt scheme. Using simulated data we showed that our algorithm provide accurate and stable results for low number of gradient directions and is favorable to direct multi-tensor fitting. We applied this algorithm to in vivo, human brain data and showed that the reconstructed orientations follow the major tracts and describe fiber intersection regions well. Furthermore, by sub-sampling the number of gradient directions we showed that plausible results can be obtained using only 12 gradient directions. The potential of this approach for reduced HARDI acquisition time is clear. In the future, we plan to deploy our new method within a tractography algorithm. In addition, accuracy and stability evaluations with respect to other reconstruction techniques, including sparsity-based methods, will be provided.

Acknowledgments. This work was made possible in part by the NIH/NIGMS Center for Integrative Biomedical Computing, 2P41 RR0112553-12.

References

1. Descoteaux, M., Angelino, E., Fitzgibbons, S., Deriche, R.: Regularized, fast, and robust analytical Q-ball imaging. Magn. Res. Med. **58**(3) (2007) 497–510
2. Tournier, J.D., Calamante, F., Connelly, A.: Robust determination of the fibre orientation distribution in diffusion MRI: Non-negativity constrained super-resolved spherical deconvolution. NeuroImage **35**(4) (2007) 1459–1472
3. Tuch, D.S., Reese, T.G., Wiegell, M.R., Makris, N., Belliveau, J.W., Wedeen, V.J.: High angular resolution diffusion imaging reveals intravoxel white matter fiber heterogeneity. Magn. Res. Med. **48**(4) (2002) 577–582
4. Weldeselassie, Y., Barmpoutis, A., Atkins, M.S.: Symmetric positive-definite cartesian tensor orientation distribution functions (CT-ODF). In Jiang, T., Navab, N., Pluim, J., Viergever, M., eds.: MICCAI'10. Volume 6361 of LNCS., Springer, Heidelberg (2010) 582–589
5. Tuch, D.S.: Q-ball imaging. Magn. Res. Med. **52**(6) (2004) 1358–1372
6. Özarslan, E., Shepherd, T.M., Vemuri, B.C., Blackband, S.J., Mareci, T.H.: Resolution of complex tissue microarchitecture using the diffusion orientation transform (DOT). NeuroImage **31**(3) (2006) 1086–1103
7. Aganj, I., Lenglet, C., Sapiro, G.: ODF maxima extraction in spherical harmonic representation via analytical search space reduction. In: MICCAI'10. Volume 6361 of LNCS. (2010) 84–91
8. Bloy, L., Verma, R.: On computing the underlying fiber directions from the diffusion orientation distribution function. In: MICCAI'08. Volume 5241 of LNCS. (2008) 1–8
9. Ghosh, A., Wassermann, D., Deriche, R.: A polynomial approach for maxima extraction and its application to tractography in hardi. In: IPMI'11. Volume 6801 of LNCS. (2011) 723–734
10. Jiao, F., Gur, Y., Johnson, C.R., Joshi, S.: Detection of crossing white matter fibers with high-order tensors and rank-k decompositions. In: IPMI'11. Volume 6801 of LNCS. (2011) 538–549

11. Schultz, T., Seidel, H.P.: Estimating crossing fibers: A tensor decomposition approach. IEEE TVCG **14**(6) (2008) 1635–1642
12. Behrens, T., Berg, H.J., Jbabdi, S., Rushworth, M., Woolrich, M.
13. Alexander, D.: Multiple-fibre reconstruction algorithms for diffusion MRI. Annals of the New York Academy of Sciences **1046** (2005) 113–133
14. Schultz, T., Westin, C.F., Kindlmann, G.: Multi-diffusion-tensor fitting via spherical deconvolution: A unifying framework. In Jiang, T., Navab, N., Pluim, J., Viergever, M., eds.: MICCAI'10. Volume 6361 of LNCS., Springer, Heidelberg (2010) 673–680
15. Rathi, Y., Malcolm, J.G., Michailovich, O., Westin, C.F., Shenton, M.E., Bouix, S.: Tensor kernels for simultaneous fiber model estimation and tractography. Magnetic Resonance in Medicine **64**(1) (2010) 138–148
16. Brachat, J., Comon, P., Mourrain, B., Tsigaridas, E.P.: Symmetric tensor decomposition. Linear Algebra and Applications **433**(11-12) (2010) 1851–1872
17. Descoteaux, M., Angelino, E., Fitzgibbons, S., Deriche, R.: Apparent diffusion coefficients from high angular resolution diffusion imaging: Estimation and applications. Magnetic Resonance in Medicine **56**(2) (2006) 395–410
18. Atkinson, K.: Numerical integration on the sphere. J. Austral. Math. Soc. **23** (1982) 332–347
19. Kaden, E., Knsche, T.R., Anwander, A.: Parametric spherical deconvolution: Inferring anatomical connectivity using diffusion MR imaging. NeuroImage **37** (2007) 474–488
20. Cook, P.A., Bai, Y., Nedjati-Gilani, S., Seunarine, K.K., Hall, M.G., Parker, G.J., Alexander, D.C.: UCL Camino Diffusion MRI Toolkit. http://cmic.cs.ucl.ac.uk/camino/ (2006)
21. Gur, Y., Jiao, F., Zhu, S.X., Johnson, C.R.: Fiber orientations assessment via symmetric tensor decomposition. In: ISBI Workshop on HARDI reconstruction, Barcelona, Spain (May 2012) http://hardi.epfl.ch/
22. Zhan, L., Leow, A.D., Jahanshad, N., Chiang, M.C., Barysheva, M., Lee, A.D., Toga, A.W., McMahon, K.L., de Zubicaray, G.I., Wright, M.J., Thompson, P.M.: How does angular resolution affect diffusion imaging measures ? NeuroImage **49**(2) (2010) 1357 – 1371